Improving emotion recognition systems by embedding cardiorespiratory coupling

PAPER

Improving emotion recognition systems by embedding cardiorespiratory coupling

IOP Publishing Physiological Measurement
Physiol. Meas. **34** (2013) 449–464 doi:10.1088/0967-3334/34/4/449

Improving emotion recognition systems by embedding cardiorespiratory coupling

Gaetano Valenza, Antonio Lanatá and Enzo Pasquale Scilingo

Department of Information Engineering and Research Center 'E. Piaggio', Faculty of Engineering, University of Pisa, Via G Caruso 16, I-56122 Pisa, Italy

E-mail: g.valenza@ieee.org, a.lanata@centropiaggio.unipi.it and e.scilingo@centropiaggio.unipi.it

Received 2 October 2012, accepted for publication 5 March 2013
Published 22 March 2013
Online at stacks.iop.org/PM/34/449

Abstract
This work aims at showing improved performances of an emotion recognition system embedding information gathered from cardiorespiratory (CR) coupling. Here, we propose a novel methodology able to robustly identify up to 25 regions of a two-dimensional space model, namely the well-known circumplex model of affect (CMA). The novelty of embedding CR coupling information in an autonomic nervous system-based feature space better reveals the sympathetic activations upon emotional stimuli. A CR synchrogram analysis was used to quantify such a coupling in terms of number of heartbeats per respiratory period. Physiological data were gathered from 35 healthy subjects emotionally elicited by means of affective pictures of the international affective picture system database. In this study, we finely detected five levels of arousal and five levels of valence as well as the neutral state, whose combinations were used for identifying 25 different affective states in the CMA plane. We show that the inclusion of the bivariate CR measures in a previously developed system based only on monovariate measures of heart rate variability, respiration dynamics and electrodermal response dramatically increases the recognition accuracy of a quadratic discriminant classifier, obtaining more than 90% of correct classification per class. Finally, we propose a comprehensive description of the CR coupling during sympathetic elicitation adapting an existing theoretical nonlinear model with external driving. The theoretical idea behind this model is that the CR system is comprised of weakly coupled self-sustained oscillators that, when exposed to an external perturbation (i.e. sympathetic activity), becomes synchronized and less sensible to input variations. Given the demonstrated role of the CR coupling, this model can constitute a general tool which is easily embedded in other model-based emotion recognition systems.

Keywords: cardiorespiratory synchronization, emotion recognition systems, heart rate variability, respiration activity, electrodermal response, weakly

coupled oscillators, dominant Lyapunov exponent, quadratic discriminant classifiers

1. Introduction

Emotion recognition systems are devised to map physiological patterns into well-defined emotional states for an automatic classification. The physiological signs include implicit and explicit emotional channels of human communication such as speech, facial expression, gesture and physiological responses (Calvo and D'Mello 2010). Focusing on biosignal-based systems, currently, the main goal is to catch the underlying dynamics of the autonomic nervous system (ANS) to effectively identify such human states. In general, the advantage of monitoring of the ANS against the central nervous system is twofold: ANS monitoring can be performed using non-invasive and wearable systems; ANS signs are less sensible to movement artifacts (e.g., heart rate variability (HRV) is more robust than the electroencephalogram). Therefore, over the last decade, several biosignals such as the electrocardiogram and the related HRV (Camm *et al* 1996, Rajendra Acharya *et al* 2006a), the respiration activity (RSP) (Lanata *et al* 2010) and the electrodermal response (EDR) (Boucsein 2011) along with ad hoc signal processing methodologies have been proposed in order to link their dynamical changes/levels to emotions. Recently, numerous automatic emotion recognition systems have been proposed involving, among others, patient–robot interactions (Swangnetr and Kaber 2012), car drivers (Katsis *et al* 2008), facial expression (Chakraborty *et al* 2009) and adaptation of game difficulty (Chanel *et al* 2011). For the sake of brevity and to avoid unnecessary repetitions, we recall the state of the art of ANS-based emotion recognition in our previous works (Valenza *et al* 2012c, 2012b) and in particular, a recent review written by Calvo and D'Mello (2010) which reports on the most relevant theories and detection systems using physiological and speech signals, face expression and movement analysis.

1.1. Affective modeling and elicitation

Two crucial parts of each emotion recognition system are represented by the modeling of emotions and elicitation methods. Each emotion recognition system, in fact, relies on a model of emotions. In the literature, one of the most common model is represented by the circumplex model of affects (CMAs) (Posner *et al* 2005) in which emotions are related to a specific region of a multiple-dimensional space. In particular, the two fundamental dimensions of CMA are conceptualized by the terms of valence and arousal, which can be intended as the two independent, predominantly subcortical systems that underlie emotions (see figure 1). Valence represents how much an emotion is felt by people as 'pleasant' or 'unpleasant', while arousal indicates the impact of the stimulus and therefore how strong the emotion is perceived. Concerning the emotional elicitation, in the light of the above modeling, a good choice is the use of an international standardized affective database whose items are categorized in terms of valence and arousal levels. The international affective picture system (IAPS) (Lang *et al* 2005) is one of the most frequently used tools having such characteristics. The IAPS is a set of 944 images having a specific emotional rating in terms of valence and arousal. The emotional ratings are based on several studies previously conducted where subjects were requested to rank these images using the self-assessment manikin (Lang *et al* 1980).

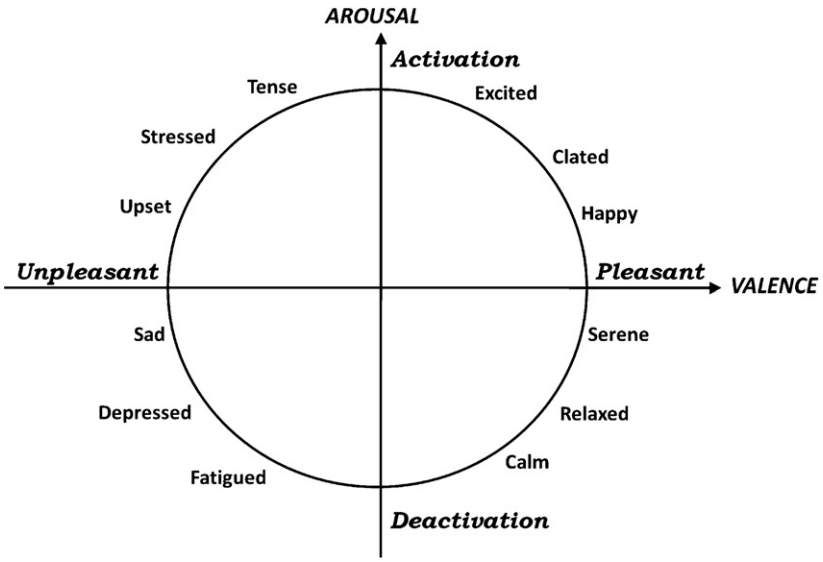

Figure 1. A graphical representation of the CMA with the horizontal axis representing the valence dimension and the vertical axis representing the arousal or activation dimension (copyright (2012) IEEE, reprinted with permission from Valenza *et al* 2012a *Front. Neuroeng.* **5** 1–7).

1.2. Background studies and current approach

In our previous work (Valenza *et al* 2012c), we studied the ANS response as a whole system by processing biosignals such as HRV and RSP, along with the EDR to implement an automatic emotion recognition system. Specifically, 35 healthy volunteers underwent a passive emotional elicitation protocol through the presentation of a set of IAPS pictures, categorized into five levels of arousal and five levels of valence, including the neutral one. As reported in section 2.1, each arousing session alternated with a neutral one and included four groups of images with a coherent valence level. Each arousing session was constituted by 20 pictures and, therefore, four consecutive images had the same level of valence. Since each image lasted for 10 s, a coherent elicitation of 40 s ensured the evaluation of the low frequencies related to the sympathetic activity, i.e. 0.04 Hz (Akselrod *et al* 1981) (see section 2.4). We applied commonly used monovariate analyses in order to extract standard features and features from nonlinear dynamic methods of analysis. The arousal and valence multi-class recognition was performed by processing the extracted feature sets through a Bayesian decision theory-based classifier which used a quadratic discriminant classifier (QDC). We found that the use of nonlinear system-derived approaches has given pivotal quantitative markers to evaluate the dynamics and predicability of ANS changes. Specifically, when nonlinearly extracted features are embedded in the mentioned affective computing system along with the linearly derived ones, the percentages of successful recognition dramatically increased (Valenza *et al* 2012c). These findings simply confirm the important role played by nonlinear and non-stationary dynamics in many physiological processes (Marmarelis 2004). This behavior, in fact, can be the result of a nonlinear frequency modulation or multi-feedback interactions among the involved biological processes. Focusing on HRV, it has been suggested that the a- and b-adrenoceptors are involved in the generation of the nonlinear HRV dynamics (seen in rats)

(Beckers *et al* 2006b). These interactions can carry out several coupling mechanisms such as bio-feedback for system regulation and synchronizations. An excellent example of coupling between the cardiovascular and respiratory systems mainly refers to the respiratory sinus arrhythmia (RSA) (Davies and Neilson 1967) and baroreflex sensitivity (BRS) (Parati *et al* 2001). By definitions of the RSA and BRS, the changes in heart rate (HR) are due to respiratory and blood pressure variations, respectively. In addition, mechanical stretch of the sinus node due to respiration (which alters the electrical properties of the sino-atrial node membrane) and respiratory phase-dependent modulation through the baroreflex information processing, etc, is present. In a previous study (Valenza *et al* 2012b), we investigated the phase synchronization between breathing patterns and HR during the mentioned IAPS passive affective elicitation. We demonstrated that respiratory and cardiac systems adapt their rhythms in response to an external emotional stimulation. In particular, when a strong affective event occurs, the CR system becomes more synchronized (reasonably due to the sympathetic and parasympathetic signaling activities). These results are in agreement with other studies pointing out that sympathetic activations can significantly increase the nonlinear CR coupling (Censi *et al* 2003). The phase synchronization was quantified by applying a bivariate analysis relying on the concept of phase synchronization of chaotic oscillators, i.e. the cardiorespiratory synchrogram (CRS) (Rosenblum *et al* 1998). This technique allowed us to estimate the synchronization ratio *m:n* as the attendance of *n* heartbeats in each *m* respiratory cycles. We observed a clearly increased synchronization during the presentation of images with significant arousal content with respect to the neutral ones, while no statistical difference has been found among sessions with slightly different arousal content. Let us conclude that an arousal affective stimulation increases the coupling between the two considered systems (Valenza *et al* 2012b).

In this work, we propose to extend our previously developed emotion recognition system (Valenza *et al* 2012c), which was based on monovariate measures, by embedding crucial bivariate information such as the cardiorespiratory (CR) coupling. The resulting all-inclusive methodology is able to robustly identify affective states using the CMA modeling approach, improving previously achieved automatic recognition of five levels of arousal and five levels of valence, including a neutral state. Therefore, the outcome of this work allows us to allocate more effectively standard and nonlinear monovariate and bivariate physiological features into 25 different affective regions in the CMA space. Moreover, with respect to the mentioned previous research activity (Valenza *et al* 2012c, 2012b), this work reports on newer theoretical and methodological aspects related to emotional elicitation and, more in general, exogenous sympathetic activation-related stimuli. In order to find theoretical foundations of emotional elicitation and to bring benefits to other model-based emotion recognition systems, in fact, we show a model of CR coupling during sympathetic elicitation using a theoretical nonlinear model. This model is a simple adaptation of the theories of weakly coupled oscillators (Rosenblum *et al* 1996, Pikovsky *et al* 1997, 2003) with external driving. The idea to model the CR system as weakly coupled self-sustained oscillators under an external perturbation is not really new. In fact, the CR synchronization has been already studied under anesthesia (Stefanovska *et al* 2000, Bartsch *et al* 2007), exercise (Kenwright *et al* 2008) or aging (Shiogai *et al* 2010), where particular emphasis was pointed out for the occurrences of transitions between synchronization regimes. Therefore, the theoretical idea behind the model is that the CR system is comprised of weakly coupled self-sustained oscillators that, when exposed to an external perturbation (i.e. sympathetic activation), becomes synchronized and less sensible to input variations. This hypothesis was experimentally proved in our previous findings relating the dominant Lyapunov exponent (Valenza *et al* 2012a) to nonlinear dynamics of the HRV. The model proposed here can be easily integrated in a more general model-based emotion recognition system.

2. Materials and methods

This section describes the experimental protocol, the data acquisition and the methodology of biosignal processing and data-mining technique that allows the arousal and valence recognition. Here, we briefly report on how the data were gathered and the rational behind the specific emotional elicitation sequence. More details can be found in Valenza *et al* (2012a, 2012b, 2012c)

2.1. Experimental protocol

A group of 35 healthy subjects (age ranged from 21 to 24), i.e. not suffering from both cardiovascular and evident mental pathologies, was asked to fill out the patient health questionnaire^{TM}. Participants whose score was lower than 5 were enrolled. The cut-off value was chosen in order to avoid the presence of either middle or severe personality disorders (Kroenke *et al* 2001). They sat on a comfortable chair while underwent a passive affective elicitation performed by using a set of images gathered from the official IAPS database. The slideshow was comprised of nine sessions of images $N, A1, N, A2, N, A3, N, A4, N$, where N is a session of six neutral images (mean valence rating 6.49, SD = 0.87, range =5.52–7.08; mean arousal rating = 2.81, SD = 0.24, range = 2.42–3.22) and A_i (with i going from 1 to 4) are sets of 20 images eliciting an increasing level of valence. For each arousal session A_i, four valence levels were defined, namely V_i, with i going from 1 to 4, from unpleasant (minimal valence rating) to pleasant (maximal arousal rating), respectively. Each image was presented for 10 s. During the visual elicitation, three physiological signals, i.e. ECG, RSP and EDR were acquired simultaneously by using the BIOPAC MP150 with a sampling rate of 250 Hz for all signals. The system included a dedicated hardware module to acquire each physiological signal. Pregelled Ag/AgCl electrodes were placed according to the Einthoven triangle configuration in order to acquire a D2 lead ECG signal with the bandwidth 0.05–35 Hz. This analogue pre-filtering stage was justified because the ECG signal was used only to extract the HRV, which refers to the variation of the time interval between consecutive heartbeats (Rajendra Acharya *et al* 2006a). Changes of electrical resistance of a piezo-resistive sensor embedded in a thoracic belt were acquired in order to obtain the respiration dynamics (Lanata *et al* 2010) (bandwidth of 0.05–10 Hz). The EDR (Boucsein 2011) was acquired by means of two Ag/AgCl electrodes positioned at the index and middle fingertips of the non-dominant hand.

2.2. Methodology of signal processing and pattern recognition

A block diagram of the proposed emotion recognition system is shown in figure 2. For each biosignal, monovariate analyses were applied in order to extract significant features using both standard and nonlinear techniques. Moreover, coupling measures by means of a bivariate analysis were extracted from the RR interval series along with the RSP. Then, the obtained feature space dimension was reduced using the principal component analysis method. Finally, features were classified using various machine learning methods (Jain and Mao 2000). QDC showed the highest recognition accuracy and consistency in both arousal and valence multi-classes.

2.3. Preprocessing

After the IAPS elicitation, all the gathered signals were preprocessed, i.e. segmented and filtered. Each signal was segmented according to the time duration of the stimulating sections.

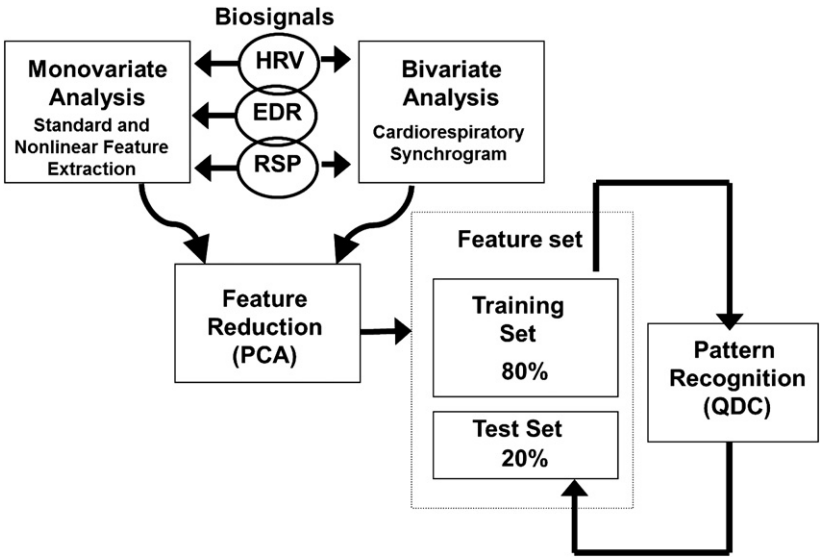

Figure 2. Block diagram representing the acquisition and processing chain.

Regarding the ECG, a moving average filter (MAF) was applied in order to extract and subtract the baseline drift. An automatic QRS detection algorithm (Pan and Tompkins 1985) was applied in order to extract the interval between two successive *R*-waves (t_{R-R}). Then, defining the HR in beats per minute as $\mathrm{HR} = \frac{60}{\mathrm{t_{R-R}}}$, the HRV was obtained. Such a time series was re-sampled at 4 Hz according to the algorithm of Berger *et al* (1986), which allowed us to deal with non-uniform RR intervals sampling. The RSP baseline was removed by means of MAF technique and, afterward, such a signal was filtered by means of a tenth-order low-pass FIR filter with a cut-off frequency of 1 Hz approximated by the Butterworth polynomial. EDR was filtered by means of a 2.5 Hz low-pass FIR filter approximated by the Butterworth polynomial. Wavelet filtering was used to split the tonic and phasic components with the bandwidth of 0–0.05 Hz, and 0.05–1–2 Hz, respectively (Ishchenko and Shev'ev 1989). The tonic component is usually associated with the baseline level of skin conductance, whereas the phasic component, superimposed on the tonic baseline level, changed according to specific external stimuli.

2.4. Monovariate analysis

In this work, several features coming from monovariate analyses were calculated. This kind of approach allowed us to extract all the possible information from a single physiological variable. Features were calculated for each stimulation session, according to the image labels. According to the current state of the art, standard features as well as features derived from the nonlinear analysis were taken into account. Standard features were derived from the time series, statistics, frequency domain and geometric analysis for the whole set of physiological signals. Concerning the HRV (Rajendra Acharya *et al* 2006a), several standard features are defined in the time and frequency domains. Time domain features included statistical parameters and morphological indexes. Defining, e.g., a time window (NN), several parameters were calculated such as simple mean value and the standard deviation of the NN intervals. Moreover, we calculated the root mean square of successive differences of

intervals and the number of successive differences of intervals which differ by more than 50 ms (pNN50% expressed as a percentage of the total number of heartbeats analyzed). Referring to morphological patterns of HRV, the triangular index was calculated. It was derived from the histogram of RR intervals into an NN window (TINN) in which a triangular interpolation was performed. The time domain methods are simple and widely used, but are unable to discriminate between sympathetic and parasympathetic activities, while an appreciable contribution is given by the frequency domain parameters. All features extracted in the frequency domain were based on the power spectral density (PSD) of the HRV (Bartoli *et al* 1985). In this work, we adopted the auto-regressive (AR) model to estimate the PSD of HRV in order to provide better frequency resolution than the nonparametric method (Bartoli *et al* 1985). We used the Burg method to obtain the AR model parameters, according to the results presented by Akaike (Akaike 1969, Boardman *et al* 2002). This method provided high resolution in frequency and yielded a stable AR model. Three main spectral components were distinguished in a spectrum calculated from short-term recordings: very low frequency (VLF) having components below 0.04 Hz, low frequency (LF) having the bandwidth from 0.04 to 0.15 Hz (Akselrod *et al* 1981) and high frequency (HF) components which are above 0.15 Hz (up to 0.4 Hz). In addition to VLF, LF and HF power, we calculated the LF/HF ratio which should give information about the sympatho-vagal balance. Specifically, LF/HF changes may indicate a shift of sympatho-vagal balance toward sympathetic predominance and reduced vagal tone (Camm *et al* 1996). From the RSP, standard measures such as the respiration rate, the mean and standard deviation of the first and second derivatives, i.e. variation of the respiration signal, standard deviation of the breathing amplitude were taken into account. The respiration rate was calculated as the frequency corresponding to the maximum spectral magnitude. Other evaluated statistical parameters included the maximum and minimum values of breathing amplitude and their difference, skewness, kurtosis and standard error of the mean (Valenza *et al* 2012c). Concerning the RSP features in the frequency domain, spectral power in the bandwidths 0–0.1 Hz, 0.1–0.2 Hz, 0.2–0.3 Hz and 0.3–0.4 Hz was also calculated (Valenza *et al* 2012c, Koelstra *et al* 2010). A standard monovariate analysis for both tonic and phasic EDR features included the same above-mentioned statistics applied to the RSP signal: rate, i.e. central frequency, mean and standard deviation of the amplitude and statistical parameters, i.e. skewness, kurtosis, SEM and mean and standard deviation of the first and second derivatives (Lang *et al* 1993). Moreover, further features were extracted only from the phasic component of EDR. More specifically, we also calculated the maximum peak and the relative latency from the beginning of the image, and spectral power in the bandwidths 0–0.1 Hz, 0.1–0.2 Hz, 0.2–0.3 Hz and 0.3–0.4 Hz (Valenza *et al* 2012c, Koelstra *et al* 2010). Other parameters from the monovariate analysis were estimated through the high-order spectral analysis, which are defined as the Fourier transform of moments or cumulants of order greater than 2. In particular, we used the two-dimensional third-order cumulant Fourier transform, called bispectrum (Mendel 1991, Nikias 1993). It quantifies the correlation among three spectral peaks, i.e. ω_1, ω_2 and $(\omega_1 + \omega_2)$ and also estimates the phase coupling among frequencies as $B(f_1, f_2) = \int\int_{t_1,t_2=-\infty}^{\infty} c_3(t_1, t_2) \exp^{-j(2\pi f_1 t_1 + 2\pi f_2 t_2)} \, \mathrm{d}t_1 \mathrm{d}t_2$ with the condition $|\omega_1|, |\omega_2| \leqslant \pi$, being $\omega = 2\pi f$, where $c_3(t_1, t_2)$ represents the third-order cumulant. In this work, the bispectral feature set extracted from the triangular non-redundant region of $B(f_1, f_2)$ was comprised of mean and variance of bispectral invariants, mean magnitude of the bispectrum and the phase entropy, normalized bispectral entropy and normalized bispectral squared entropy (see Chua *et al* (2010) for a detailed review).

Several nonlinear measures were also carried out along with the extraction of standard morphological and spectral features (Rajendra Acharya *et al* 2006b). Even if the physiological meaning of these features is still unclear, this choice was motivated since they have been

revealed as an important quantifier of cardiovascular control dynamics, mediated by the ANS. We refer to nonlinear measures as features extracted from the phase space (or state space). More specifically, once the phase space is estimated (by means of the so-called embedding procedure), we evaluated the parameters that seemed to be subjected to an ANS modulation. An effective method seen as an extension of autocorrelation function is the recurrence plot (RP) (Marwan *et al* 2007). It is a graph which shows all those times at which a state of the dynamical system recurs. In other words, the RP reveals all the times when the phase space trajectory visits roughly the same area in the phase space. In this study, such an area was chosen as a sphere having an optimized ray (Schinkel *et al* 2008). The RP representation is a squared matrix $N \times N$, whose element $R_{i,j}$ is set to 1 when a state at time i recurs also at time j, and 0 otherwise. Following the above description, we used the recurrence quantification analysis (RQA) (Zbilut and Webber Jr 2006), which is a method of nonlinear data analysis which quantifies the number and duration of recurrences of a dynamical system presented by its state space trajectory. The quantification of RP can be based either on evaluating diagonal lines to estimate chaos–order transitions or on vertical (horizontal) lines to estimate chaos–chaos transitions. In this work, the following RQA features were calculated (Zbilut and Webber Jr 2006): recurrence rate ($\mathrm{Rr} = \frac{1}{\mathrm{N}^2}\sum_{\mathrm{i,j}=1}^{\mathrm{N}} \mathrm{R_{i,j}}$), determinism ($\mathrm{DET} = \frac{\sum_{\mathrm{l}=\mathrm{l}_{\min}}^{\mathrm{N}} \mathrm{lP(l)}}{\sum_{\mathrm{i,j}=1}^{\mathrm{N}} \mathrm{R_{i,j}}}$, where $P(l)$ is the histogram of the lengths l of the diagonal lines), laminarity ($\mathrm{LAM} = \frac{\sum_{\upsilon=\upsilon_{\min}}^{\mathrm{N}} \upsilon \mathrm{P}(\upsilon)}{\sum_{\upsilon=1}^{\mathrm{N}} \upsilon \mathrm{P}(\upsilon)}$), trapping time ($\mathrm{TT} = \frac{\sum_{\upsilon=\upsilon_{\min}}^{\mathrm{N}} \upsilon \mathrm{P}(\upsilon)}{\sum_{\upsilon=\upsilon_{\min}}^{\mathrm{N}} \upsilon \mathrm{P}(\upsilon)}$), ratio ($\mathrm{RATIO} = \frac{\mathrm{DET}}{\mathrm{Rr}}$), averaged diagonal line length ($L = \frac{\sum_{l=l_{\min}}^{N} lP(l)}{\sum_{l=l_{\min}}^{N} P(l)}$), entropy ($\mathrm{ENTR} = -\sum_{\mathrm{l}=\mathrm{l}_{\min}}^{\mathrm{N}} \mathrm{p(l)} \ln \mathrm{p(l)}$) and longest diagonal line ($L_{\max} = \max(\{l_i;\, i = 1, ..., N_l\}$, where N_l is the number of diagonal lines in the RP). The evaluation of such RQA parameters is justified by their associated meaning in describing a dynamical system. In fact, Rr, L and DET are associated with the probability and predicability that a specific state will recur, whereas LAM and TT are related to the laminarity of the dynamical system, i.e. how long the system remains in a specific state. The ENTR quantifies the complexity of the deterministic structure in the system, and RATIO and $L_{\max}$ are simple measures of recurrence structures.

In addition, we used the detrended fluctuation analysis (DFA), which is a method for determining the statistical self-affinity of a signal. DFA was introduced by Peng *et al* (1994) and represents an extension of the (ordinary) fluctuation analysis, which is affected by non-stationarities. Concerning the calculation, each series was first integrated and, then, divided into boxes of equal length n. In each box of length n, a least-squares line was fit to the data in order to detrend the integrated time series. Finally, the root-mean-square fluctuation of this integrated and detrended time series was calculated as $F(n) = \sqrt{\frac{1}{N}\sum_{k=1}^{N} [y(k) - y_n(k)]^2}$.

2.5. Bivariate analysis

The novelty of this work is also related to the inclusion of CR coupling measures in an emotion recognition system based only on features coming from the monovariate analysis. Hereinafter, such a coupling refers to the phase synchronization occurring between the CR systems. Formally, given the phase dynamics of the two systems, ϕ_1 and ϕ_2, the synchronization is defined as $\phi_{1,2} = n\phi_1 - m\phi_2 <= \text{const.}$, regardless of the amplitudes. m and n are some integers that describe the phase locking ratio. It is noteworthy mentioning that the phase synchronization needs the estimation of the instantaneous phases at least for the slower oscillating signal. In our case, the instantaneous RSP phase was calculated by means of the Hilbert transform (Boashash 1992). To quantify the CR coupling, we employed the CRS

technique, recently proposed by Schafer *et al* (1998, 1999). Concepts of phase synchronization of chaotic oscillators are adopted to analyze the irregular non-stationary bivariate data. In the general case of *m:n* synchronization, such a structure appears if we relate the phases of the heart beats to the beginning of *m* adjacent respiratory cycles:

$$\varphi(t_k) = \frac{\phi_r(t_k) \bmod (2\pi m)}{2\pi}, \tag{1}$$

where ϕ_r refers to the instantaneous phase of the respiratory signal and t_k is the time where the *R*-peak in the *k*th heartbeat occurs and hence the phase of the heart rhythm increases by 2π. ϕ_r is calculated by means of the Hilbert transformation (Rosenblum *et al* 1996). By plotting the relative phases φ as a function of t_k, CRS shows *n* horizontal stripes within *m* respiratory cycles whenever an*m:n* phase synchronization occurs. For our emotion recognition system, we calculated the percentage of synchronized signals for each session of each subject. The following physiological-plausible synchronization ratios $n : m$ were included into the feature space: $1 : 6$, $1 : 5$, $1 : 4$, $1 : 3$, $2 : 9$, $2 : 7$, $3 : 11$, $3 : 10$, $3 : 8$.

2.6. Feature reduction and pattern recognition

In this work, a feature reduction technique was applied in order to reduce the obtained high dimension of the feature space. We implemented the well-known principal component analysis (PCA) method, which belongs to the class of feature projection methods. The PCA projects high-dimensional data to a lower dimensional space through a linear transformation of original feature values. These output variables are ordered according to decreasing variance and are called principal components. PCA uses the eigenvalues and eigenvectors generated by the correlation matrix to rotate the original dataset along the direction of maximum variance. Accordingly, we have implemented the above general description by means of the singular value decomposition (Jolliffe 2002). After the feature reduction, the pattern recognition phase was performed. In this work, a quadratic Bayes normal classifier (Duda *et al* 2001, Valenza *et al* 2012c) (also called QDC) was used because of the best performance obtained (Valenza *et al* 2012c). The performance of the classification is presented in the form of confusion matrix. The generic element r_{ij} of the confusion matrix indicates how many times in percentage a pattern belonging to the class i was classified as belonging to the class j. A more diagonal confusion matrix corresponds to a higher degree of classification. The matrix has to be read by columns. The training phase is carried out on 80% of the feature dataset (subset from 28 subjects) while the testing phase to the remaining seven subjects. We performed 40-fold cross-validation steps in order to obtain unbiased classification results, i.e. it allowed us to consider the Gaussian distribution of classification results, which can be therefore described as mean and standard deviation among the 40 confusion matrices obtained. Below, the classifier is described in detail. QDC uses a supervised learning method which determines the parameters based on available knowledge.

3. Experimental results

Experimental results on emotion recognition report on the capability of the classifier to discriminate the five different arousal and five different valence classes. Relying on the CMA model of emotion (Posner *et al* 2005), in fact, it is possible to associate a certain emotion with a specific combination of arousal and valence levels (see an example in figure 1). Therefore, in further applications, given a certain elicitation, it would be possible to evaluate the proper arousal and valence levels whose combination results in one of the 25 different regions of the CMA. Since this paper points out the role of CR coupling, the feature set obtained by means of

Table 1. Comparison of the arousal level recognition accuracy for the feature set α and the proposed feature set β.

QDC	Dataset	N	A1	A2	A3	A4
N	α	**100 ± 0.0**	0.0 ± 0.0	0.0 ± 0.0	0.0 ± 0.0	0.0 ± 0.0
	β	**100 ± 0.0**	5.4 ± 9.6	1.4 ± 5.7	4.9 ± 11.1	8.1 ± 13.1
A1	α	0.0 ± 0.0	**100 ± 0.0**	0.0 ± 0.0	0.0 ± 0.0	0.0 ± 0.0
	β	0.0 ± 0.0	**94.6 ± 9.6**	0.0 ± 0.0	0.0 ± 0.0	0.0 ± 0.0
A2	α	0.0 ± 0.0	0.0 ± 0.0	**92.9 ± 10.7**	0.0 ± 0.0	4.6 ± 8.8
	β	0.0 ± 0.0	0.0 ± 0.0	**98.6 ± 5.7**	0.0 ± 0.0	0.0 ± 0.0
A3	α	0.0 ± 0.0	0.0 ± 0.0	5.3 ± 8.4	**82.9 ± 14.2**	19.3 ± 16.7
	β	0.0 ± 0.0	0.0 ± 0.0	0.0 ± 0.0	**95.1 ± 11.1**	0.0 ± 0.0
A4	α	0.0 ± 0.0	0.0 ± 0.0	1.8 ± 4.8	17.1 ± 14.2	**76.1 ± 16.9**
	β	0.0 ± 0.0	0.0 ± 0.0	0.0 ± 0.0	0.0 ± 0.0	**91.9 ± 13.1**

Table 2. Comparison of the valence level recognition accuracy for the feature set α and the proposed feature set β.

QDC	Dataset	N	V1	V2	V3	V4
N	α	**96.8 ± 7.5**	3.9 ± 6.4	0.0 ± 0.0	0.0 ± 0.0	0.0 ± 0.0
	β	**100 ± 0.0**	3.1 ± 4.5	0.0 ± 0.0	0.0 ± 0.0	0.0 ± 0.0
V1	α	3.2 ± 7.5	**96.1 ± 6.4**	0.0 ± 0.0	0.0 ± 0.0	0.0 ± 0.0
	β	0.0 ± 0.0	**94.7 ± 4.5**	0.0 ± 0.0	0.0 ± 0.0	0.0 ± 0.0
V2	α	0.0 ± 0.0	0.0 ± 0.0	**87.1 ± 11.1**	0.0 ± 0.0	18.6 ± 11.2
	β	0.0 ± 0.0	2.2 ± 4.5	**91.7 ± 9.8**	0.0 ± 0.0	0.0 ± 0.0
V3	α	0.0 ± 0.0	0.0 ± 0.0	0.0 ± 0.0	**100 ± 0.0**	0.0 ± 0.0
	β	0.0 ± 0.0	0.0 ± 0.0	2.0 ± 9.8	**90.1 ± 4.7**	5.1 ± 9.8
V4	α	0.0 ± 0.0	0.0 ± 0.0	12.9 ± 11.1	0.0 ± 0.0	**81.4 ± 11.2**
	β	0.0 ± 0.0	0.0 ± 0.0	6.3 ± 9.8	8.9 ± 4.7	**94.9 ± 9.8**

monovariate analysis only was taken as a reference and labeled as α. Such a reference feature set is comprised of all the monovariate features extracted by the HRV, RSP and EDR signals as described in section 2.4. The proposed feature set, which represents the union set of α and the features coming from the bivariate analysis, was labeled as β. After the feature extraction phase, the PCA algorithm was applied to each dataset. We stopped the reduction process when the cumulative variance reached 95%. The discrimination results are shown in tables 1 and 2 for the arousal and the valence, respectively. The QDC performances are expressed in the form of a confusion matrix calculated after 40 steps of cross-fold validation. The neutral elicitation is labeled as N, the arousal levels as A_i with $i = \{1, 2, 3, 4\}$ and the valence levels as V_i with $i = \{1, 2, 3, 4\}$. It is straightforward to note that the inclusion of the CR features improves the classification accuracy in both the arousal and valence recognition problems.

4. Modeling the CR coupling during arousal elicitation

The methodology proposed in this work for the effective emotion recognition system definitely deals with monovariate and bivariate nonparametric techniques. In fact, given the experimental data, i.e. ANS signals, we applied several transformations in order to obtain a reliable data-driven feature set able to train our automatic classification algorithm. However, other emotion recognition systems could be based on parametric approaches, i.e. using cardiovascular models having state variables related to the specific kind of elicitation. Therefore, based on our previous

findings, we here propose an equation model of CR coupling during sympathetic elicitation. This model is a simple adaptation of the theories of weakly coupled oscillators (Rosenblum *et al* 1996, Pikovsky *et al* 1997, 2003) with external driving. Accordingly, this model can constitute a general tool to be easily embedded in other model-based emotion recognition systems. In a previous study (Valenza *et al* 2012a), we evaluated the HRV nonlinear dynamics through the well-known dominant Lyapunov exponents (DLEs) (Ruelle 1979). The DLE calculation followed the approach proposed by Rosenstein *et al* (1993) which ensures reliable values of DLE even in short datasets. We found that, starting from positive values kept also during the neutral elicitation sessions, the DLE became negative during the arousal session with statistical significance ($p < 0.05$). The repeated intra-subject analysis confirmed how the DLE was positive during neutral sessions and negative during the arousal sessions (Valenza *et al* 2012a). Therefore, it is reasonable to hypothesize a relationship between the DLE and the CR synchronization findings, especially from a biophysics point of view. In fact, the physiological signals recorded during the presentation of pictures with arousal contents present a clear loss of DLE (with the change of the sign) as well as a CR phase synchronization increase (Valenza *et al* 2012b). The connection between DLE and synchronization is well characterized for nonlinear and also chaotic systems (Rosenblum *et al* 1996, Pikovsky *et al* 1997). In fact, if two or more nonlinear oscillatory processes (e.g., heart beat and respiratory activity) are weakly coupled, they can become phase synchronized and such a synchronization manifests itself in the Lyapunov spectrum of the system (Rosenblum *et al* 1996). Such a coupling leads to a decrease of the $n\phi_1 - m\phi_2$ differences. Moreover, considering an external force (i.e. perturbation) applied to the systems, the DLE is expected to be negative, as a result of a stable value of the phase with respect to the phase of the external force, in the time domain (Pikovsky *et al* 1997). The novelty of this model regards only the fact that it is possible to adapt the nonlinear model of weakly coupled oscillators to the CR system relying on previously defined equations. Let us consider the Fourier representation of the HRV as the weighted summation of complex functions having frequencies $f_{\mathrm{HRV}} = \omega_{\mathrm{HRV}}/2\pi$. Likewise, let us consider the respiration dynamics in the frequency domain but with only one component, which corresponds to the respiratory frequency $f_{\mathrm{RSP}} = \omega_{\mathrm{RSP}}/2\pi$. Therefore, the HRV and RSP phase dynamics can be written as follows:

$$\dot{\phi}_{\mathrm{HRV}} = \omega_{\mathrm{HRV}} + F(\mathrm{HRV}, \mathrm{t}) \tag{2}$$

$$\dot{\phi}_{\mathrm{RSP}} = \omega_{\mathrm{RSP}} + F(\mathrm{RSP}, \mathrm{t}), \tag{3}$$

where $F(\mathrm{HRV}, \mathrm{t})$ and $F(\mathrm{RSP}, \mathrm{t})$ stand for factors depending on the amplitude of HRV and RSP, respectively. When the two oscillators become coupled, we can write

$$\begin{cases} \dot{\phi}_{\mathrm{HRV}} = \omega_{\mathrm{HRV}} + F_{\mathrm{HRV}}(\mathrm{HRV}, \mathrm{t}) + \varepsilon \mathrm{G}(\phi_{\mathrm{RSP}}, \phi_{\mathrm{HRV}}, \psi) \\ \dot{\phi}_{\mathrm{RSP}} = \omega_{\mathrm{RSP}} + F_{\mathrm{RSP}}(\mathrm{RSP}, \mathrm{t}) + \varepsilon \mathrm{G}(\phi_{\mathrm{HRV}}, \phi_{\mathrm{RSP}}, \psi). \end{cases} \tag{4}$$

The simplest non-trivial case is given by $G(\phi_{\mathrm{HRV}}, \phi_{\mathrm{RSP}}, \psi) = \sin[(\phi_{\mathrm{RSP}} + \phi_{\mathrm{HRV}}) - \psi] = \sin(\Delta\phi_{\mathrm{CR}})$, where $\Omega = \mathrm{d}\psi/\mathrm{d}t$ represents the dominant oscillation of an external stimulus (i.e. external force and perturbation). Equation (4) becomes

$$\frac{\mathrm{d}\Delta\phi_{\mathrm{CR}}}{\mathrm{d}t} = \{\omega_{\mathrm{HRV}} + \omega_{\mathrm{RSP}} - \Omega\} + 2\varepsilon \sin(\Delta\phi_{\mathrm{CR}}) + \{F(\mathrm{HRV}, \mathrm{t}) + \mathrm{F}(\mathrm{RSP}, \mathrm{t})\}. \tag{5}$$

This equation is similar to the simple Langevin equation describing phase locking of periodic oscillators in the presence of noise (Stratonovich 1967). In our experimental framework, it is possible to consider a specific $\Omega = \Omega_{\mathrm{GN}} = \mathrm{d}\psi_{\mathrm{IAPS}}/\mathrm{d}t$ assuming its amplitude as a function of the arousal level and the frequency of elicitation of the $\dot{\phi}_{\mathrm{HRV}}$ and $\dot{\phi}_{\mathrm{RSP}}$ systems as a function

of the valence level. It is possible to write the formal solution of this equation if we assume the $\{F\,(\mathrm{HRV, t}) + \mathrm{F(RSP, t)}\}$ to be Gaussian δ-correlated:
$\{F\,(\mathrm{HRV, t}) + \mathrm{F(RSP, t)}\}\{\mathrm{F(HRV, t')} + \mathrm{F(RSP, t')}\} = 2\mathrm{D}\delta\,(\mathrm{t} - \mathrm{t'})$. Therefore, it could be solved by using the Fokker–Planck equation where the main quantities that would characterize such a synchronization are, precisely, the averaged frequency $\langle \Delta\dot{\phi}_{\mathrm{CR}} \rangle$ and the Lyapunov exponent. Briefly, the Fokker–Planck equation can be written as follows:

$$\frac{\partial W}{\partial \Delta\phi_{\mathrm{CR}}} = \frac{\partial}{\partial \Delta\phi_{\mathrm{CR}}}[(\{\omega_{\mathrm{HRV}} + \omega_{\mathrm{RSP}} - \Omega\} + 2\varepsilon \sin(\Delta\phi_{\mathrm{CR}}))W] + D\frac{\partial^2 W}{\partial \Delta\phi_{\mathrm{CR}}^2}. \tag{6}$$

Taking the Fourier representation of the stationary solution:

$$W\,(\Delta\phi_{\mathrm{CR}}) = \sum W_k \mathrm{e}^{\mathrm{i}k\Delta\phi_{\mathrm{CR}}}. \tag{7}$$

We can write the continuous-fraction representation of the first Fourier mode as shown in the following equation:

$$W_1 = \frac{(2\pi)^{-1}}{\frac{2\mathrm{i}}{\varepsilon}(\{\omega_{\mathrm{HRV}} + \omega_{\mathrm{RSP}} - \Omega\} - \mathrm{iD}) + \frac{1}{\frac{2\mathrm{i}}{\varepsilon}(\{\omega_{\mathrm{HRV}} + \omega_{\mathrm{RSP}} - \Omega\} - \mathrm{i2D}) + \cdots}}. \tag{8}$$

Therefore, the CR synchronization is mainly characterized by means of the averaged frequency

$$\langle \Delta\dot{\phi}_{\mathrm{CR}} \rangle = \{\omega_{\mathrm{HRV}} + \omega_{\mathrm{RSP}} - \Omega\} + 2\pi\varepsilon \mathrm{Im}(\mathrm{W}_1) \tag{9}$$

and the Lyapunov exponent

$$\left\langle \frac{d \ln \delta\,\Delta\phi_{\mathrm{CR}}}{\mathrm{d}t} \right\rangle = -2\pi\varepsilon \mathrm{Re}(\mathrm{W}_1). \tag{10}$$

5. Conclusion and discussion

In conclusion, a novel and effective emotion recognition system has been reported. The innovative combination of bivariate and monovariate measures improved the system in terms of recognition accuracy. Specifically, monovariate analyses were applied in order to extract significant features using both standard and nonlinear techniques to each of the three considered ANS-related biosignals, i.e. HRV, RSP and EDR. Bivariate measures, related to the CR phase synchronization, were included into the system. Therefore, the HRV along with the RSP information was engaged in the CRS analysis in which the synchronization was expressed as the ratio *m:n* explaining the presence of *n* heartbeats in each *m* respiratory cycle. The obtained feature space dimension was reduced using the PCA method and a QDC algorithm performed the pattern recognition phase. We tested the ability of our system during an ad hoc experimental study involving 35 healthy subjects who were passively emotionally elicited using standardized images. Such affective stimuli were characterized by the circumplex model of affects (CMAs) (Posner *et al* 2005) in which the affective states are conceptualized by the terms of valence and arousal. Valence represents the extent to which an emotion is perceived as being pleasant or unpleasant. Arousal indicates the intensity of the emotion. Accordingly, the stimuli were presented as images gathered from the international affective picture system (IAPS) having five levels of arousal and five levels of valence, including a neutral reference level. The experimental timeline foresaw the alternation of arousal and neutral blocks. During the elicitation, the three peripheral physiological signals were simultaneously acquired. Results are very satisfactory. Despite the reference set α, the proposed feature set β gave a recognition accuracy greater than 90% for all classes in both arousal and valence discriminations. Moreover, the performed cross-validation process, i.e. randomizing

the subjects for training and test sets, ensured that the classification was independent from the specific subjects involved. Although the proposed methodology definitely goes beyond the state of the art, we report less performances in identifying one arousal class, i.e. $A1$, and two valence classes, i.e. $V1$ and $V3$. From the literature, it is possible to consider the CMA plane as an orthonormal space in which each point is a combination of arousal and valence values. Hence, our classification findings allowed the fine identification of 25 regions. Although this is a great achievement, it is noteworthy mentioning that they may not represent 25 different emotional states. In principle, it is possible to apply our approach to any stimulus acting on the CR systems that produces a sympathetic activation (a statistically significant sympathetic activation was found during the arousal sessions by evaluating changes in the sympatho-vagal balance, i.e. LF/HF ratio of the HRV (Valenza *et al* 2012b)). From a physiological point of view, the crucial role of CR coupling is provided by considering the overlapping of power spectra of the two interacting systems, the cardiovascular and the respiratory one. It has been shown that, due to interaction, the peaks of such power spectra may become practically equal, and the peak frequencies become closer (Landa and Perminov 1985, Zhang *et al* 1997), and it has been interpreted as the synchronization of the systems quantified by means of cross-correlation functions (Landa and Perminov 1985), respiration response curve (Zhang *et al* 1997) and multivariate spectral decomposition (Baselli *et al* 1997). This principle could be the ideally theoretical explanation of the respiratory sinus arrhythmia (RSA) (Davies and Neilson 1967) in which great components of the HRV spectrum are consistent with the respiratory frequency f_{RSP}. Moreover, these experimental findings and theorization are in agreement with the *chaos-destroying* synchronization, i.e. when a periodic external force acts on a chaotic system, it destroys chaos and a periodic regime appears (Kuznetsov *et al* 1985). In the case of an irregular forcing, the driven system follows the behavior of the force (Kocarev *et al* 1993), which has been experimentally demonstrated by the evaluation of the ANS response as a whole system (Valenza *et al* 2012c). In such a case, in fact, the CR system seems to cope with the visual elicitation by producing ANS linear and nonlinear markers able to follow the stimulus changes. In a previous study (Valenza *et al* 2012c), we demonstrated how the use of nonlinear system-derived approaches is very important for an effective emotion recognition system for both arousal and valence recognitions. When nonlinearly extracted features are embedded in the affective computing system along with the linearly derived ones, in fact, the percentages of successful recognition dramatically increased (Valenza *et al* 2012c). These encouraging results prompted us to extend the study of nonlinear dynamics also for the CR system interactions. In fact, nowadays, it is well accepted that the cardiovascular system and its relationship with respiration is truly a complex system. Therefore, nonlinearities and nonlinear measures should be taken into account in its modeling and analysis (Grassberger and Procaccia 1983). In the current literature, it is not new that techniques derived from nonlinear dynamics and chaos theory may be of complementary value in identifying patterns and mechanisms in biological systems that are not detectable with traditional statistics based on linear models (Nicolini *et al* 2012, Beckers *et al* 2006a). Moreover, based on the experimental evidence on DLE and CRS, a theoretical nonlinear model on cardiopulmonary oscillators has been reported. It relies on the previously defined theory of weakly coupled oscillators (Rosenblum *et al* 1996, Pikovsky *et al* 1997, 2003) driven by external force. We hypothesized that the external force is given to the CR systems through the ANS activity modulation on the sympathetic and parasympathetic nerves. Although the chaotic behavior cannot be demonstrated in such a bio-system because of the strong physiological noise, the theory reported here aims at giving a useful tool for the assessment of the CR phase synchronization and the DLE changes in HRV.

Acknowledgments

The research leading to these results has received partial funding from the European Union Seventh Framework Programme (FP7/2007-2013) under grant agreement no. 247777 (PSYCHE).

References

Akaike H 1969 Fitting autoregressive models for prediction *Ann. Inst. Stat. Math.* **21** 243–7

Akselrod S *et al* 1981 Power spectrum analysis of heart rate fluctuation: a quantitative probe of beat-to-beat cardiovascular control *Science* **213** 220–2

Bartoli F, Baselli G and Cerutti S 1985 Ar identification and spectral estimate applied to the RR interval measurements *Int. J. Biomed. Comput.* **16** 201–15

Bartsch R, Kantelhardt J, Penzel T and Havlin S 2007 Experimental evidence for phase synchronization transitions in the human cardiorespiratory system *Phys. Rev. Lett.* **98** 54102

Baselli G, Porta A, Rimoldi O, Pagani M and Cerutti S 1997 Spectral decomposition in multichannel recordings based on multivariate parametric identification *IEEE Trans. Biomed. Eng.* **44** 1092–101

Beckers F, Verheyden B and Aubert A E 2006a Aging and nonlinear heart rate control in a healthy population *Am. J. Physiol.* **290** H2560–70

Beckers F, Verheyden B, Ramaekers D, Swynghedauw B and Aubert A E 2006b Effects of autonomic blockade on non-linear cardiovascular variability indices in rats *Clin. Exp. Pharmacol. Physiol.* **33** 431–9

Berger R, Akselrod S, Gordon D and Cohen R 1986 An efficient algorithm for spectral analysis of heart rate variability *IEEE Trans. Biomed. Eng.* **33** 900–4

Boardman A, Schlindwein F, Rocha A and Leite A 2002 A study on the optimum order of autoregressive models for heart rate variability *Physiol. Meas.* **23** 325

Boashash B 1992 Estimating and interpreting the instantaneous frequency of a signal. i. fundamentals *Proc. IEEE* **80** 520–38

Boucsein W 2011 *Electrodermal Activity* (Berlin: Springer)

Calvo R and D'Mello S 2010 Affect detection: an interdisciplinary review of models, methods, and their applications *IEEE Trans. Affective Comput.* **1** 18–37

Camm A *et al* 1996 Heart rate variability: standards of measurement, physiological interpretation, and clinical use *Circulation* **93** 1043–65

Censi F, Calcagnini G, Strano S, Bartolini P and Barbaro V 2003 Nonlinear coupling among heart rate, blood pressure, and respiration in patients susceptible to neuromediated syncope *Ann. Biomed. Eng.* **31** 1097–105

Chakraborty A, Konar A, Chakraborty U and Chatterjee A 2009 Emotion recognition from facial expressions and its control using fuzzy logic *IEEE Trans. Syst. Man Cybern.* A **39** 726–43

Chanel G, Rebetez C, Bétrancourt M and Pun T 2011 Emotion assessment from physiological signals for adaptation of game difficulty *IEEE Trans. Syst. Man Cybern.* A **41** 1052–63

Chua K, Chandran V, Acharya U and Lim C 2010 Application of higher order statistics/spectra in biomedical signals—a review *Med. Eng. Phys.* **32** 679–89

Davies C and Neilson J 1967 Sinus arrhythmia in man at rest *J. Appl. Physiol.* **22** 947–55

Duda R, Hart P and Stork D 2001 *Pattern Classification* 2nd edn (New York: John Wiley)

Grassberger P and Procaccia I 1983 Measuring the strangeness of strange attractors *Physica* D **9** 189–208

Ishchenko A and Shev'ev P 1989 Automated complex for multiparameter analysis of the galvanic skin response signal *Biomed. Eng.* **23** 113–7

Jain A and Mao R 2000 Statistical pattern recognition: a review *IEEE Trans. Pattern Anal. Mach. Intell.* **22** 4–37

Jolliffe I 2002 *Principal Component Analysis* vol 2 (New York: Wiley)

Katsis C, Katertsidis N, Ganiatsas G and Fotiadis D 2008 Toward emotion recognition in car-racing drivers: a biosignal processing approach *IEEE Trans. Syst. Man Cybern.* A **38** 502–12

Kenwright D, Bahraminasab A, Stefanovska A and McClintock P 2008 The effect of low-frequency oscillations on cardio-respiratory synchronization *Eur. Phys. J.* B **65** 425–33

Kocarev L, Shang A and Chua L 1993 Transition in dynamical regime by driving: a method of control and synchronization of chaos *Technical Report* UCB/ERL M93/32 (University of California : Electronics Research Laboratory, College of Engineering)

Koelstra S, Yazdani A, Soleymani M, Mühl C, Lee J, Nijholt A, Pun T, Ebrahimi T and Patras I 2010 Single trial classification of EEG and peripheral physiological signals for recognition of emotions induced by music videos *Proc. 2010 Int. Conf. on Brain Informatics* (Berlin: Springer-Verlag) pp 89–100

Kroenke K, Spitzer R and Williams J 2001 The phq-9 *J. Gen. Intern. Med.* **16** 606–13

Kuznetsov Y, Landa P, Ol'Khovoi A and Perminov S 1985 Relationship between the amplitude threshold of synchronization and the entropy in stochastic self-excited systems *Sov. Phys.—Dokl.* **30** 221–2

Lanata A *et al* 2010 Comparative evaluation of susceptibility to motion artifact in different wearable systems for monitoring respiratory rate *IEEE Trans. Inform. Technol. Biomed.* **14** 378–86

Landa P and Perminov S 1985 Interaction of periodic and stochastic oscillations *Radiophys. Quantum Electron.* **28** 284–7

Lang P, Bradley M and Cuthbert B 2005 International affective picture system (IAPS): digitized photographs, instruction manual and affective ratings *Technical Report* A-6 (Florida, FL: University of Florida)

Lang P, Greenwald M, Bradley M and Hamm A 1993 Looking at pictures: affective, facial, visceral, and behavioral reactions *Psychophysiology* **30** 261–73

Lang P *et al* 1980 Behavioral treatment and bio-behavioral assessment: computer applications *Technology in Mental Health Care Delivery Systems* (New York: Ablex) pp 119–37

Marmarelis V 2004 *Nonlinear Dynamic Modeling of Physiological Systems* (New York: Wiley)

Marwan N, Carmen Romano M, Thiel M and Kurths J 2007 Recurrence plots for the analysis of complex systems *Phys. Rep.* **438** 237–329

Mendel J 1991 Tutorial on higher-order statistics (spectra) in signal processing and system theory: theoretical results and some applications *Proc. IEEE* **79** 278–305

Nicolini P, Ciulla M, Asmundis C, Magrini F and Brugada P 2012 The prognostic value of heart rate variability in the elderly, changing the perspective: from sympathovagal balance to chaos theory *Pacing Clin. Electrophysiol.* **35** 621–37

Nikias C 1993 *Higher-Order Spectral Analysis: A Nonlinear Signal Processing Framework* (Englewood Cliffs, NJ: PTR Prentice-Hall)

Pan J and Tompkins W 1985 A real-time QRS detection algorithm *IEEE Trans. Biomed. Eng.* **32** 230–6

Parati G, Rienzo M and Mancia G 2001 Dynamic modulation of baroreflex sensitivity in health and disease *Ann. New York Acad. Sci.* **940** 469–87

Peng C, Buldyrev S, Havlin S, Simons M, Stanley H and Goldberger A 1994 Mosaic organization of dna nucleotides *Phys. Rev.* E **49** 1685

Pikovsky A, Rosenblum M and Kurths J 2003 *Synchronization: A Universal Concept in Nonlinear Sciences* vol 12 (Cambridge: Cambridge University Press)

Pikovsky A, Rosenblum M, Osipov G and Kurths J 1997 Phase synchronization of chaotic oscillators by external driving *Physica* D **104** 219–38

Posner J, Russell J and Peterson B 2005 The circumplex model of affect: an integrative approach to affective neuroscience, cognitive development, and psychopathology *Dev. Psychopathol.* **17** 715–34

Rajendra Acharya U, Paul Joseph K, Kannathal N, Lim C and Suri J 2006a Heart rate variability: a review *Med. Biol. Eng. Comput.* **44** 1031–51

Rajendra Acharya U, Paul Joseph K, Kannathal N, Lim C and Suri J 2006b Heart rate variability: a review *Med. Biol. Eng. Comput.* **44** 1031–51

Rosenstein M, Collins J and De Luca C 1993 A practical method for calculating largest Lyapunov exponents from small data sets *Physica* D **65** 117–34

Rosenblum M, Kurths J, Pikovsky A, Schafer C, Tass P and Abel H 1998 Synchronization in noisy systems and cardiorespiratory interaction *IEEE Eng. Med. Biol. Mag.* **17** 46–53

Rosenblum M, Pikovsky A and Kurths J 1996 Phase synchronization of chaotic oscillators *Phys. Rev. Lett.* **76** 1804–7

Ruelle D 1979 Sensitive dependence on initial condition and turbulent behavior of dynamical systems *Ann. New York Acad. Sci.* **316** 408–16

Schafer C, Rosenblum M, Abel H and Kurths J 1999 Synchronization in the human cardiorespiratory system *Phys. Rev.* E **60** 857

Schafer C, Rosenblum M, Kurths J and Abel H 1998 Heartbeat synchronized with ventilation *Nature* **392** 239

Schinkel S, Dimigen O and Marwan N 2008 Selection of recurrence threshold for signal detection *Eur. Phys. J.* **164** 45–53

Shiogai Y, Stefanovska A and McClintock P 2010 Nonlinear dynamics of cardiovascular ageing *Phys. Rep.* **488** 51–110

Stefanovska A, Haken H, McClintock P, Hožič M, Bajrović F and Ribarič S 2000 Reversible transitions between synchronization states of the cardiorespiratory system *Phys. Rev. Lett.* **85** 4831–4

Stratonovich R 1967 *Topics in the Theory of Random Noise: General Theory of Random Processes, Nonlinear Transformations of Signals and Noise* vol 1 (London: Gordon and Breach)

Swangnetr M and Kaber D B 2012 Emotional state classification in patient–robot interaction using wavelet analysis and statistics-based feature selection *IEEE Trans. Hum. Mach. Syst.* **43** 63–75

Valenza G, Allegrini P, Lanatà A and Scilingo E 2012a Dominant Lyapunov exponent and approximate entropy in heart rate variability during emotional visual elicitation *Front. Neuroeng.* **5** 1–7

Valenza G, Lanatà A and Scilingo E 2012b Oscillations of heart rate and respiration synchronize during affective visual stimulation *IEEE Trans. Inform. Technol. Biomed.* **16** 683–90

Valenza G, Lanata A and Scilingo E 2012c The role of nonlinear dynamics in affective valence and arousal recognition *IEEE Trans. Affective Comput.* **3** 237–49

Zbilut J and Webber C Jr 2006 *Recurrence Quantification Analysis* (New York: Wiley)

Zhang P Z, Tapp W N, Reisman S S and Natelson B H 1997 Respiration response curve analysis of heart rate variability *IEEE Trans. Biomed. Eng.* **44** 321–5